Blue Light Emitting Ir(III) Compounds for OLEDs - New Insights into Ancillary Ligand Effects on the Emitting Triplet State

Andreas F. Rausch,[†] Mark E. Thompson,[‡] and Hartmut Yersin*,[†]

Universität Regensburg, Institut für Physikalische und Theoretische Chemie, 93053 Regensburg, Germany, and University of Southern California, Department of Chemistry, Los Angeles, California 90089

Received: March 13, 2009

The sky-blue emitting phosphorescent compound Ir(4,6-dFppy)$_2$(acac) (FIracac) doped into different matrices is studied under ambient conditions and at cryogenic temperatures on the basis of broadband and high-resolution emission spectra. The emitting triplet state is found to be largely of metal-to-ligand charge transfer (MLCT) character. It is observed that different polycrystalline and amorphous hosts distinctly affect the properties of the triplet. Moreover, a comparison of FIracac with the related Ir(4,6-dFppy)$_2$(pic) (FIrpic), differing only by the ancillary ligand, reveals obvious changes of properties of the emitting state. These observations are explained by different effects of acac and pic on the Ir(III) d-orbitals. In particular, the occupied frontier orbitals, strongly involving the t_{2g}-manifold, and their splitting patterns are modified differently. This influences spin−orbit coupling (SOC) of the emitting triplet state to higher-lying ^{1,3}MLCT states. As a consequence, zero-field splittings, radiative decay rates, and phosphorescence quantum yields are changed. The important effects of SOC are discussed qualitatively and are related to the emission properties of the individual triplet substates, as determined from highly resolved spectra. The results allow us to gain a better understanding of the impact of SOC on the emission properties with the aim to develop more efficient triplet emitters for OLEDs.

1. Introduction

During the last several years, Ir(III) compounds have attracted much interest as highly efficient emissive dopants in organic light emitting diodes (OLEDs).[1−4] The strong spin−orbit coupling (SOC) induced by the heavy metal center allows both singlet and triplet excitons to be used in an electroluminescence process, which leads to up to four times higher internal electroluminescence quantum yield than achievable with fluorescent emitters (triplet harvesting effect).[5,6] The nature of the lowest excited state and thus the emission properties can be tuned by a careful choice of the cyclometallating chromophoric ligand.[2,7−10] Another possibility of influencing these properties is achievable by a change of the nonchromophoric ligand, the so-called ancillary or spectator ligand.[11−15] Because of its high triplet energies, the spectator ligand is not directly involved in the emission process, but it can shift the metal d-orbitals and alter their splitting patterns. Thus, the metal orbital participation in the excited state and the efficiency of spin−orbit coupling (SOC) can be influenced.[11,12] Until now, no detailed investigations of ancillary ligand effects on the electronic properties of Ir(III) compounds based on optical high-resolution spectroscopy have been carried out.

In this study, we spectroscopically investigate the lowest excited state T_1 of the sky-blue emitting compound iridium(III)bis[2-(4′,6′-difluorophenyl)pyridinato-N,C$^{2'}$]-acetylacetonate (Ir(4,6-dFppy)$_2$(acac), FIracac)[16] (inset of Figure 1) in different host materials, focusing on electronic properties of the lowest triplet state, such as zero-field splittings and individual decay times of the T_1 substates. The results reveal that the emitting triplet state, being largely of MLCT character, exhibits a significant dependence on the host environment. The observed behavior is comparable to the situation found recently for Ir(4,6-dFppy)$_2$(pic) (FIrpic).[17] This latter compound, which differs only in the ancillary ligand from FIracac, represents a famous OLED emitter material[4,16,18,19] and has already been spectroscopically studied in detail.[17,20] High-resolution optical spectra at cryogenic temperatures and ambient temperature investigations allow a detailed comparison of the two emitters and reveal an insight into the influences of the ancillary ligands acac and pic on the properties of the emitting state. It is shown that the observed dissimilarities can be rationalized by different d-orbital involvements in the lowest triplet states of the respective compounds. By the exchange of acac to pic, the efficiency of spin−orbit coupling (SOC) of the T_1 substates to higher-lying singlets and triplets of MLCT character is altered and, thus, the emission

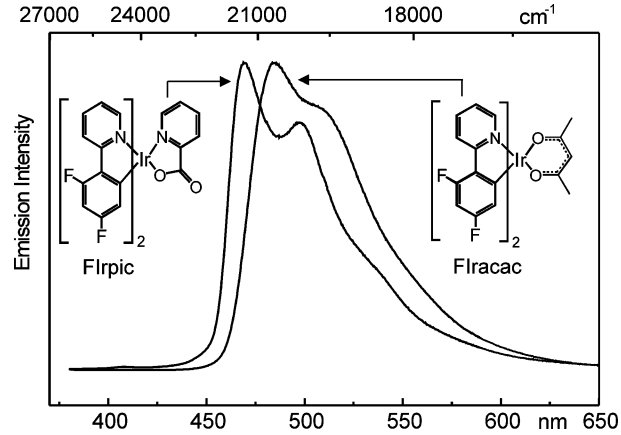

Figure 1. Emission of FIracac and FIrpic in CH_2Cl_2 (λ_{exc} = 300 nm) at T = 300 K. The insets show the structures of the compounds.

* To whom correspondence should be addressed. E-mail: hartmut.yersin@chemie.uni-regensburg.de.
† Universität Regensburg.
‡ University of Southern California.

10.1021/jp902261c CCC: $40.75
Published on Web 04/28/2009

TABLE 1: Emission Properties of FIracac and FIrpic at Ambient Temperature in Different Solvents/Matrices

	Ir(4,6-dFppy)$_2$(acac) (FIracac)			Ir(4,6-dFppy)$_2$(pic) (FIrpic)		
	CH_2Cl_2	THF	PMMA	CH_2Cl_2	THF	PMMA
λ_{max} [nm]	484	486	479	470	471	468
τ_{em} [μs]	1.0	1.2	1.2	1.9	1.8	1.7
ϕ_{PL}	0.64	0.67	0.74	0.83	0.84	0.89
$k_r{}^a$ [s^{-1}]	6.4×10^5	5.6×10^5	6.2×10^5	4.4×10^5	4.6×10^5	5.2×10^5
$k_{nr}{}^a$ [s^{-1}]	3.6×10^5	2.8×10^5	2.2×10^5	0.9×10^5	0.9×10^5	0.6×10^5

[a] Radiative and nonradiative rate constants are calculated from the quantum yields and emission decay times according to eq 1.

properties are also changed. Further, we address shortly the differences in the nonradiative decay behavior of the two compounds.

2. Experimental Section

Synthesis. FIracac and FIrpic were synthesized according to the procedures described in refs 12 and 21, respectively.

Spectroscopy. Spectroscopic measurements were carried out with FIracac and FIrpic dissolved in CH_2Cl_2 and THF (tetrahydrofuran), respectively, at concentrations of about 10^{-5} mol/L. Doped PMMA (polymethylmethacrylate) films were prepared by dissolving the compounds ($\sim$1 wt %) and PMMA in CH_2Cl_2. Subsequently, the solutions were spin-coated on a quartz plate. Emission spectra at 300 K were measured with a steady-state fluorescence spectrometer (Jobin Yvon Fluorolog 3). Luminescence quantum yields were determined with an integrating sphere (Labsphere, 4P-GPS-033-SL), which exhibits a highly reflective Spectralon inside coating. The estimated relative error is about $\pm$0.10. Fluid solutions were degassed by at least three pump−freeze−thaw cycles with a final vapor pressure at 77 K of $\sim 10^{-5}$ mbar, while the PMMA films were measured under a nitrogen atmosphere. Experiments at low temperature were carried out in a He cryostat (Cryovac Konti Cryostat IT) in which He gas flow, He pressure, and heating were controlled. A pulsed Nd:YAG laser (IB Laser Inc., DiNY pQ 02) with a pulse width of about 7 ns was applied as excitation source for emission decay time measurements, using the third harmonic at 355 nm (28170 cm^{-1}). For recording site-selective emission and excitation spectra, a pulsed dye laser (Lambdaphysik Scanmate 2C) was operated, using Coumarin 102. The spectra were measured with an intensified CCD camera (Princeton PIMAX) or with a cooled photomultiplier (RCA C7164R) attached to a triple spectrograph (S&I Trivista TR 555). Decay times were registered using a FAST Comtec multichannel scaler PCI card with a time resolution of 250 ps.

3. Results and Discussion

3.1. Spectroscopic Introduction. Figure 1 shows the emission spectra of FIracac and FIrpic dissolved in CH_2Cl_2, measured at ambient conditions. The emission of FIracac has its maximum at 484 nm (20 660 cm^{-1}). In deaerated solution, the decay time constant is 1.0 μs and the phosphorescence quantum yield amounts to 64%. These values do not change remarkably when the compound is investigated in THF (Table 1). However, when doped into a rigid PMMA host, a blue shift of the emission is observed. This is a well-known phenomenon for compounds that exhibit a significant charge transfer with the corresponding electronic transition.[22] Further, the emission quantum yield is higher in PMMA than in fluid solution. The emission of FIrpic is slightly more structured and lies at higher energy, in CH_2Cl_2 its maximum is found at 470 nm (21 280 cm^{-1}). Further, the emission decay time (1.9 μs) is longer and the photoluminescence quantum yield (83%) is higher than that of FIracac.

The ambient temperature emission spectra of both compounds are significantly less resolved than, for example, the spectrum of Ir(btp)$_2$(acac) (btp$^-$ = (2-benzothienyl)-pyridinate).[2,23] This indicates a considerably larger MLCT character in the emitting state of FIracac and FIrpic because a distinct involvement of the metal orbitals in the corresponding transitions is usually connected with pronounced metal−ligand vibrational satellites with energies below 600 cm^{-1} relative to the electronic origin. Usually, this leads to a smearing out of the emission spectrum at room temperature.[24,25]

Photophysical data of FIracac and FIrpic in different hosts measured at ambient temperature are summarized in Table 1. The emission quantum yields and decay times found for FIrpic closely match the values reported for other solvents and host materials.[26] A detailed comparison of the two compounds will be carried out in section 3.3. The radiative and the nonradiative rate constants are calculated according to the equation

$$\phi_{PL} = k_r \tau_{em} = \frac{k_r}{k_r + k_{nr}} \quad (1)$$

wherein ϕ_{PL} is the photoluminescence quantum yield and τ_{em} is the emission decay time. k_r and k_{nr} represent the radiative and the nonradiative decay rates, respectively.

3.2. Triplet Substates and Energy Level Diagram of FIracac in CH_2Cl_2 Based on High-Resolution Spectroscopy. The ambient temperature spectra are very broad due to homogeneous and inhomogeneous broadening effects especially in fluid solution. Thus, only a crude characterization of the emitting triplet state is possible. However, detailed information can be obtained from highly resolved emission and excitation spectra at cryogenic temperatures. Therefore, FIracac is investigated in polycrystalline CH_2Cl_2 down to 1.7 K. In particular, this host has proven to be a suitable matrix for high-resolution spectroscopy of Ir(III) complexes.[17,23] Comparable to the situation found for FIrpic[17] and Ir(btp)$_2$(acac),[23] several discrete sites (emitter molecules in specific host environments) are found. The spectra of the sites are characterized by narrow emission lines. When excited with UV light, also a broad background is observed, which is due to an additional inhomogeneous distribution of emitter molecules in the applied matrix (Figure 2).

In Figure 3, site-selectively excited emission spectra and a site-selectively detected excitation spectrum are displayed for the region of the electronic 0−0 transitions of the prominent site of lowest energy, which is labeled as Site A in Figure 2. The emission spectrum measured at $T = 1.7$ K (part b of Figure 3) shows one intense line at 21 025 cm^{-1}, which is the line of highest energy at that temperature. Therefore, it is assigned as electronic 0−0 transition from the lowest T_1 substate I to the singlet ground state S_0. With increasing temperature, an additional line appears at 21 041 cm^{-1}. This line results from the electronic 0−0 transition II $\rightarrow$ 0. With further temperature increase, line II gains intensity, but even at $T = 15$ K, line I is still the most intense one. Further, the peaks become broader.

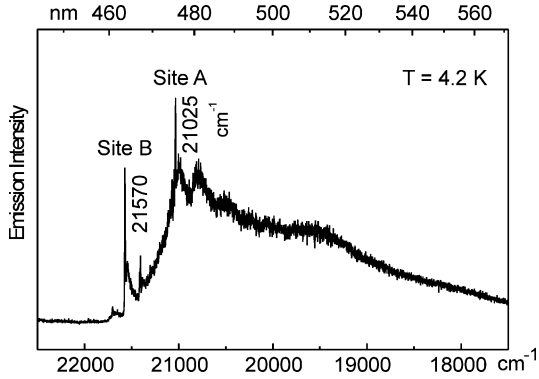

Figure 2. Emission spectrum of FIracac in CH_2Cl_2 at $T = 4.2$ K after excitation at 355 nm. Several discrete sites are observed together with a relatively intense inhomogeneous background. The two most intense sites are labeled as Site A and Site B.

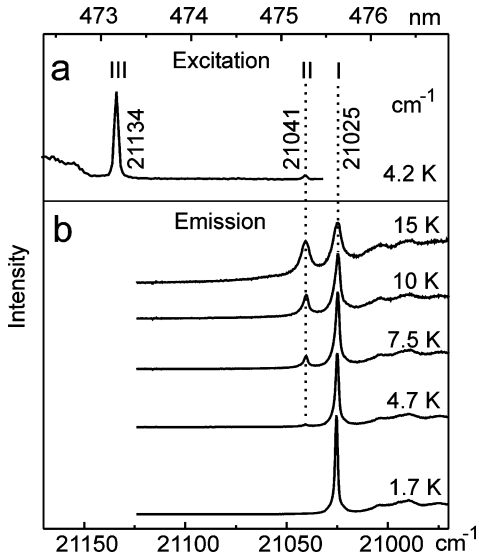

Figure 3. Site-selective spectra of the region of the $T_1 \leftrightarrow S_0$ 0−0 transitions of site A of FIracac in CH_2Cl_2. (a) Site-selectively detected excitation spectrum recorded at $T = 4.2$ K. The emission is detected at 21 025 cm^{-1} (electronic 0−0 transition I → 0). (b) Emission spectra recorded after selective excitation of the 0−0 transition of substate III at 21 134 cm^{-1}.

This effect is frequently observed and can be explained by the involvement of local low-energy vibrations of the dopant in its matrix cage, which exhibit slightly different energies in the electronic ground state compared to the excited state. The corresponding 1−1 transitions, which occur at higher temperature, lie near to but not exactly at the energy of the 0−0 transition. This causes a line broadening.

The excitation spectrum for the energy range of the electronic origins is reproduced in part a of Figure 3. Two excitation lines at 21 041 and 21 134 cm^{-1} can be observed. The weak peak at 21 041 cm^{-1} is in resonance with the corresponding emission line as expected for an electronic 0−0 transition. Because no other line is observable in the relevant energy range, the high-energy line at 21 134 cm^{-1} is assigned to the 0−0 transition from the singlet ground S_0 state to the highest T_1 substate III. Interestingly, no additional line that might correspond to an electronic origin of a higher lying triplet state can be detected within the range of 1500 cm^{-1} to higher energy. Recently, Zhang, Ma, and co-workers predicted the occurrence of two close-lying triplet states T_2 and T_3 on the basis of TDDFT calculations.[27] However, their calculations do not yet include

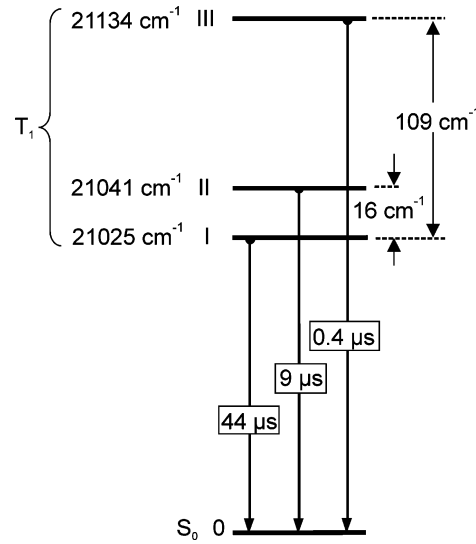

Figure 4. Energy level diagram and decay times for the T_1 substates I, II, and III of site A of FIracac in CH_2Cl_2.

spin−orbit coupling, which might lead to significant energy shifts between the lowest triplets.

The intensity ratio obtained from the excitation spectrum shown in part a of Figure 3 reveals that the transition 0 → III is by a factor of 21 more allowed than the transition 0 → II. Thus, the transition between triplet substate III and the singlet ground state S_0 carries by far the highest oscillator strength (radiative allowedness) and mainly governs the emission properties at ambient temperature. This result is further supported by an analysis of the individual decay times of the triplet substates as obtained from the temperature dependence of the thermalized emission decay time. (Here not discussed in detail, but compare e.g. refs 28−30). The corresponding data and the results obtained from the high-resolution measurements are summarized in the energy level diagram as depicted in Figure 4. According to an empirical ordering scheme,[31−33] the T_1 state of the main site of FIracac in CH_2Cl_2 with a total zero-field splitting of 109 cm^{-1} can be assigned to be largely of MLCT character.

For the ratio of rate constants k_{III}/k_{II} ($k = {}^1/_\tau$) as determined from the temperature dependence of the thermalized emission decay time, a value of 22 is found, which is in good agreement with the ratio determined from the corresponding excitation peaks in part a of Figure 3. This behavior is indicative of very similar radiative deactivation mechanisms of the substates II and III and indicates an emission quantum yield of almost 100% for both substates at cryogenic temperatures.

For completeness, it is mentioned that the other intense discrete site of FIracac in CH_2Cl_2, labeled as Site B in Figure 2, exhibits different zero-field splittings with $\Delta E_{II-I} = 13$ cm^{-1} and $\Delta E_{III-I} = 92$ cm^{-1}. As explained below, such deviations between different sites are not unusual for Ir(III) compounds. Interestingly, for both compounds, FIracac and FIrpic,[17] the sites of lowest energy exhibit the highest zero-field splittings. However, for $Ir(btp)_2(acac)$ in CH_2Cl_2 a manifold of sites was characterized, but a correlation between the emission energy and the zero-field splitting was not observed.[23]

3.3. Comparison of FIracac and FIrpic − Influence of Ancillary Ligands. In Table 1, ambient temperature data of FIracac are compared to corresponding data of FIrpic, whereas Table 2 summarizes T_1 state properties of both compounds as determined at cryogenic temperatures.

The emitting triplet state of FIrpic lies about 700 cm^{-1} (~0.09 eV) higher in energy than the triplet of FIracac (Tables 1 and

TABLE 2: Energy Separations and Individual Decay Times of the Triplet Substates I, II, and III of FIracac in Different Matrices; T_1 State Properties of FIrpic in CH_2Cl_2 are also Displayed

	FIracac			FIrpic[b]
	CH_2Cl_2[a]	THF	PMMA	CH_2Cl_2
0−0 transition 0 ↔ I [cm^{-1}]	21 025			21 738
ΔE_{II-I} [cm^{-1}]	16	10−15	10−15	9
ΔE_{III-I} [cm^{-1}]	109	80−125	75−120	76
τ_I [μs]	44	68	74	47
τ_{II} [μs]	9	9−19	10−20	21
τ_{III} [μs]	0.4	0.2−0.5	0.3−0.6	0.3

[a] Site A. [b] From ref 17, main site.

2). Although this energy difference is not large, it is still important for the realization of a deeper-blue light emitting material. The observed energy shift is ascribed to different influences of the ancillary ligands acac and pic on the Ir(III) d-orbitals. In particular, the coordination of the central metal ion to nitrogen leads to a stronger bond than the coordination to oxygen.[34] DFT calculations performed on both compounds support this assumption because the Ir−N bond length to picolinate was determined to be substantially shorter than the Ir−O bond length to acetylacetonate.[27] Therefore, a higher mean ligand field strength is indicated for the pic ligand compared to the acac ligand. As consequence, the occupied d-orbitals of the t_{2g} manifold experience on average[34] a larger energy stabilization in FIrpic than in FIracac. The situation is schematically depicted in Figure 5.

Interestingly, our schematic model is supported by the oxidation potentials of the compounds. They amount to 0.90 and 0.74 V (measured vs ferrocene) for FIrpic and FIracac, respectively.[35,36] On the other hand, the π^*-orbitals of the chromophoric 4,6-dFppy ligands are − in this first order model − expected to remain almost unchanged. (Compare also ref 11) Thus, the d−π^* energy separations are expected to be larger for FIrpic than for FIracac. These energy differences will also be displayed in the corresponding ^{1}MLCT and ^{3}MLCT states, and indeed this trend is found experimentally for the transition energies.

In this simple consideration, we assume that the occupied π-orbitals of the chromophoric 4,6-dFppy ligands lie at the same energy for both compounds and are located below of the d-orbitals, but in energy proximity (compare for example refs 37−39). Thus, the close-lying d- and π-orbitals of adequate symmetry will combine to molecular orbitals. Obviously, the d−π mixing and thus the π-contribution to the occupied frontier orbitals is expected to be larger for FIrpic because of the smaller d−π energy separation compared to FIracac. Consequently, the "pureness" of MLCT character of the resulting states will become smaller with enhanced LC contributions to the emitting state. This mixing effect will also reduce the effectiveness of spin−orbit coupling, which is dominantly carried by the metal d-orbital contributions. Therefore, it is expected that the photophysical properties which are related to the effectiveness of SOC, such as ZFSs, radiative decay rates, and emission quantum yields, are strongly influenced by the discussed mixings. Indeed, this trend is observed. ZFSs (Table 2) and average radiative rates at ambient conditions (Table 1) are larger for FIracac (with less π-admixtures to the occupied d-orbitals and thus less LC admixtures to the emitting state) than for FIrpic.

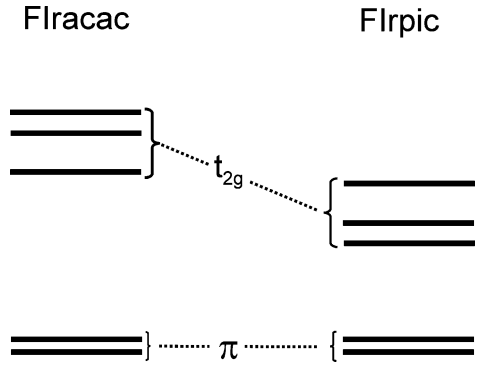

Figure 5. Schematic energy pattern for the occupied d-orbitals of the t_{2g} manifold and occupied π-orbitals of the chromophoric ligands. The diagram manifests trends to illustrate the discussion given in the text.

The basic model presented above can be extended, if an additional effect, which can also modify zero-field splittings and radiative decay rates, is taken into account. Thus, further insights into triplet state properties are provided. We want to illustrate this issue by discussing the relevant SOC routes on the basis of interacting energy states.

A quantitative description of the triplet state properties of organometallic compounds based on quantum mechanical calculations including SOC is still very difficult (e.g., compare ref 40). However, the effects of SOC on the ZFS of the T_1 term and on the radiative decay rates of the triplet substates can be illustrated by formulas based on second-order perturbation theory. The energy $E(i)$ of one specific triplet substate i of T_1 (with i = I, II, III) can be expressed by[20,32,41]

$$E(i) = E_{T_1} + \sum_{T_n} \frac{|\langle \varphi_{T_n(j)} | \hat{H}_{SO} | \varphi_{T_1(i)} \rangle|^2}{E_{T_1} - E_{T_n}} + \sum_{S_n} \frac{|\langle \varphi_{S_n} | \hat{H}_{SO} | \varphi_{T_1(i)} \rangle|^2}{E_{T_1} - E_{S_n}} \quad (2)$$

whereas the radiative rate constant $k_r(i)$ of T_1 substate i for the transition to the electronic ground-state S_0 is given by[20,32,42]

$$k_r(i) = \text{const} \times \bar{\nu}^3 \times \left| \sum_{S_n} \frac{\langle \varphi_{S_n} | \hat{H}_{SO} | \varphi_{T_1(i)} \rangle}{E_{T_1} - E_{S_n}} \times \langle \varphi_{S_0} | e\vec{r} | \varphi_{S_n} \rangle \right|^2 \quad (3)$$

wherein $\hat{H}_{SO}$ is the SOC Hamiltonian, and E_{T_1}, E_{S_n}, and E_{T_n} are the unperturbed energies of the lowest triplet and of higher lying singlet and triplet states S_n and T_n, respectively. $T_n(j)$ characterizes a substate j of T_n. φ_{S_n} and $\varphi_{T_n(j)}$ represent the corresponding wave functions. In particular, they must have the same symmetry representation as the wave function $\varphi_{T_1(i)}$ of T_1 substate i, otherwise the matrix elements in eqs 2 and 3 vanish. $\bar{\nu}$ represents the transition energy between the excited and the ground state and $e\vec{r}$ is the electric dipole operator.

The SOC matrix elements are usually different for the three T_1 substates. This leads to different energy stabilizations and thus to the ZFS as well as to different radiative rates. In particular, the most prominent effects of SOC are determined by the most proximate energy states because the corresponding energy denominators in eqs 2 and 3 are smaller than for states of higher energy. Obviously, substantial SOC in these complexes is only induced by the central metal d-orbitals. This means that the SOC matrix elements can only attain significant values, if (i) both the substates of the lowest triplet and the mixing-in states are MLCT states or contain at least some MLCT character and if (ii) the mixing MLCT states involve *different* d-orbitals.[20,32,43] Thus, the most prominent

SOC admixtures to the substates of the lowest ^{3}MLCT state are related to couplings to the energetically most proximate ^{1,3}MLCT states that stem from different d-orbitals, whereas couplings to ^{1}LC states will be inefficient with respect to SOC. Especially, the next nearest frontier orbital with significant d-character, for example HOMO−1, will be highly important. If the corresponding d-orbital (which results from the t_{2g} manifold) experiences an energy shift, for example induced by lowering the symmetry or by exchanging the ancillary ligand, the mixings governing SOC will be altered. In particular, it is expected that the strongly asymmetric pic ligand induces a different splitting of the three occupied d-orbitals than the more symmetric acac ligand. This is schematically depicted in Figure 5. From the experimental results, we can conclude that FIracac exhibits a d-orbital pattern with two more proximate frontier orbitals (HOMO and HOMO−1) than occurring for FIrpic because just this situation will result in higher SOC efficiencies and thus a larger ZFS and a higher average radiative decay rate for FIracac. Interestingly, recent calculations on both compounds support this model. A smaller energy separation between HOMO and HOMO−1 was found for FIracac than for FIrpic.[27]

For completeness, it is mentioned that in pseudo-octahedrally coordinated compounds the orbitals of the t_{2g} manifold usually lie relatively close in energy.[37,38,44] Therefore, even small shifts of these energies/splittings will have distinct impact on the SOC efficiencies and therefore on the emission properties due to changes of the energy denominators in eqs 2 and 3 (compare also next section).

In summary, both the amount of d−π mixing and the individual pattern of the occupied frontier orbitals will influence zero-field splittings and radiative decay rates. Both quantum-mechanical effects let us predict a larger ZFS and radiative decay rate for FIracac than for FIrpic − just as experimentally observed (Tables 1 and 2).

It is remarked that nonradiative processes are not included in the model presented. However, they cannot be neglected because an increase of the nonradiative deactivation rate k_{nr} can lead − despite higher radiative rates − to a lower photoluminescence quantum yield. This behavior is observed for FIracac (Table 1). The higher nonradiative rate for this compound compared to FIrpic can be related to differently effective deactivation processes by molecular vibrations. In particular, the higher symmetry of FIracac might be connected with a delocalization of the lowest triplet state over the two chromophoric ligands, whereas in the asymmetric FIrpic the T_1 state will probably be confined to only one chromophoric ligand (as is also indicated by DFT calculations[27]). In the latter case, the number of vibrational modes that can deactivate nonradiatively is substantially lower. Interestingly, investigations on Os(II) compounds have shown that complexes with one chromophoric ligand tend to exhibit higher photoluminescence quantum yields than corresponding complexes with two chromophoric ligands.[45] However, we cannot rule out that vibrational modes of acac and pic, respectively, might also affect the radiationless deactivation. Further, thermal population of quenching metal centered (MC, dd*) states might have an additional impact on the emission quantum yield. Because of the lower ligand field strength of acac compared to pic, the dd* states are supposed to lie at somewhat lower energy in FIracac than in FIrpic. Thus, population of those quenching dd* states at room temperature might be more pronounced in FIracac.

3.4. Matrix Effects on SOC and on the Triplet State Properties. In several investigations at high resolution, it was observed that the T_1 state properties of Ir(III) compounds depend on the individual site and on the host material.[23,32,43,46] For example, for FIrpic in CH_2Cl_2, the T_1 states of two discrete sites have been studied in detail and were found to exhibit distinctly different zero-field splittings and substate decay times.[17] Also, for host materials in which the Ir(III) compounds give only broadband spectra (even at cryogenic temperatures), the zero-field splitting values and individual substate decay times are not discrete but are spread over specific ranges.[17,47] Upper and lower limits for these ranges can be determined by a procedure based on temperature dependent emission decay time measurements, as described in ref 17. A corresponding behavior is also found for FIracac when doped into THF and PMMA, respectively. In these hosts, only broadband spectra are obtained and it is observed that the ZFS values and T_1 sublevel decay times are significantly spread (Table 2). Such effects occur in polycrystalline hosts[17,23,32] as well as in amorphous matrices.[47] However, the degree of the spread can vary (Table 2). Interestingly, the values observed for the discrete sites in CH_2Cl_2 (section 3.2) closely correspond to the ranges observed for THF and PMMA. The observed behavior of a variation of T_1 state properties is rationalized with a sensitivity of the MLCT states of Ir(III) complexes on the host environment (matrix cage).[17] Changes affected by the local environment can, for example, alter the complex geometry by steric effects and influence the energies of the metal d-orbitals − in a similar manner as discussed above for the exchange of the ancillary ligand. As a consequence, the energies of the corresponding MLCT states are also altered and the energy denominators in eqs 2 and 3 are affected. According to these influences, the emitter molecules experience differently effective SOCs and thus exhibit different ZFSs and average radiative decay rates. It is remarked that matrix induced changes of the d−π mixtures, as discussed in section 3.3, may also be of importance.

4. Summary and Conclusions

Photophysical properties of Ir(4,6-dFppy)$_2$(acac) (FIracac) and Ir(4,6-dFppy)$_2$(pic) (FIrpic) are investigated in detail, focusing on the emission behavior. Both compounds are highly emissive and their lowest excited electronic states are assigned to be largely of ^{3}MLCT character. The ancillary ligands acac and pic have distinct (but indirect) influence on the excited state properties by modifying the splittings and energy positions of the occupied frontier orbitals. These are largely of central metal d-character and stem from the t_{2g}-manifold. In a schematic and simple model, we relate especially the splitting pattern/energy separations of the frontier orbitals HOMO and HOMO−1 to the effectiveness of spin−orbit coupling of the T_1 substates to higher lying ^{1,3}MLCT states. Thus, relations between simple MO considerations and detailed photophysical properties such as zero-field splittings, radiative decay rates, and so forth become to survey. It is even possible to understand, qualitatively, how a purely organic host environment can modify the effectiveness of SOC. These influences are of particular importance for octahedrally coordinated complexes with emitting states of ^{3}MLCT character, especially for Ir(III) complexes, which are most suited for OLED applications.

Because of the higher MLCT character in the emitting state, FIracac should represent a better OLED material than FIrpic. However, a slightly lower energy of the emitting ^{3}MLCT state makes the compound less well suited for highly desired blue emitting OLEDs than FIrpic. Further, the photoluminescence quantum yield of FIracac is smaller than that of FIrpic, that is FIracac is distinctly more influenced by nonradiative decay processes. This is presumably due to the involvement of both

chromophoric 4,6-dFppy-ligands in the emitting state of the more symmetric FIracac. Thus, new efforts for the design of OLED triplet emitters should not only take into account a high MLCT character in the emitting state but also complex symmetry and matrix effects.

Acknowledgment. The *Bundesministerium für Bildung und Forschung (BMBF)* is gratefully acknowledged for providing the funding of this investigation. We thank the *German Academic Exchange Service (DAAD)* for financial support of the exchange program of the University of Regensburg with the University of Southern California.

References and Notes

(1) *Highly Efficient OLEDs with Phosphorescent Materials*; Yersin, H., Ed.; Wiley-VCH: Weinheim, 2008.
(2) Tamayo, A. B.; Garon, S.; Sajoto, T.; Djurovich, P. I.; Tsyba, I. M.; Bau, R.; Thompson, M. E. *Inorg. Chem.* **2005**, *44*, 8723.
(3) Yang, C.-H.; Cheng, Y.-M.; Chi, Y.; Hsu, C.-J.; Fang, F.-C.; Wong, K.-T.; Chou, P.-T.; Chang, C.-H.; Tsai, M.-H.; Wu, C.-C. *Angew. Chem., Int. Ed.* **2007**, *46*, 2418.
(4) Su, S.-J.; Gonmori, E.; Sasabe, H.; Kido, J. *Adv. Mater.* **2008**, *20*, 4189.
(5) Adachi, C.; Baldo, M. A.; Thompson, M. E.; Forrest, S. R. *J. Appl. Phys.* **2001**, *90*, 5048.
(6) Yersin, H. *Top. Curr. Chem.* **2004**, *241*, 1.
(7) Lamansky, S.; Djurovich, P.; Murphy, D.; Abdel-Razzaq, F.; Kwong, R.; Tsyba, I.; Bortz, M.; Mui, B.; Bau, R.; Thompson, M. E. *Inorg. Chem.* **2001**, *40*, 1704.
(8) Tamayo, A. B.; Alleyne, B. D.; Djurovich, P. I.; Lamansky, S.; Tsyba, I.; Ho, N. N.; Bau, R.; Thompson, M. E. *J. Am. Chem. Soc.* **2003**, *125*, 7377.
(9) Williams, J. A. G.; Wilkinson, A. J.; Whittle, V. L. *Dalton Trans.* **2008**, *16*, 2081.
(10) Hwang, F.-M.; Chen, H.-Y.; Chen, P.-S.; Liu, C.-S.; Chi, Y.; Shu, C.-F.; Wu, F.-I.; Chou, P.-T.; Peng, S.-M.; Lee, G.-H. *Inorg. Chem.* **2005**, *44*, 1344.
(11) Li, J.; Djurovich, P. I.; Alleyne, B. D.; Yousufuddin, M.; Ho, N. N.; Thomas, J. C.; Peters, J. C.; Bau, R.; Thompson, M. E. *Inorg. Chem.* **2005**, *44*, 1713.
(12) Li, J.; Djurovich, P. I.; Alleyne, B. D.; Tsyba, I.; Ho, N. N.; Bau, R.; Thompson, M. E. *Polyhedron* **2004**, *23*, 419.
(13) Chin, C. S.; Eum, M.-S.; Kim, S. Y.; Kim, C.; Kang, S. K. *Eur. J. Inorg. Chem.* **2007**, *3*, 372.
(14) Di Censeo, D.; Fantacci, S.; de Angelis, F.; Klein, C.; Evans, N.; Kalyanasundaram, K.; Bolink, H. J.; Grätzel, M.; Nazeeruddin, M. K. *Inorg. Chem.* **2008**, *47*, 980.
(15) Chou, P.-T.; Chi, Y. *Chem.—Eur. J.* **2007**, *13*, 380.
(16) Adachi, C.; Kwong, R. C.; Djurovich, P. I.; Adamovich, V.; Baldo, M. A.; Thompson, M. E.; Forrest, S. R. *Appl. Phys. Lett.* **2001**, *79*, 2082.
(17) Rausch, A. F.; Thompson, M. E.; Yersin, H. *Inorg. Chem.* **2009**, *48*, 1928.
(18) Su, S.-J.; Sasabe, H.; Takeda, T.; Kido, J. *Chem. Mater.* **2008**, *20*, 1691.
(19) Vecchi, P. A.; Padmaperuma, A. B.; Qiao, H.; Sapochak, L. S.; Burrows, P. E. *Org. Lett.* **2006**, *8*, 4211.
(20) Rausch, A. F.; Homeier, H. H. H.; Djurovich, P. I.; Thompson, M. E.; Yersin, H. *Proc. SPIE—Int. Soc. Opt. Eng.* **2007**, *6655*, 66550F.
(21) Lamansky, S.; Thompson, M. E.; Adamovich, V.; Djurovich, P. I.; Adachi, C.; Baldo, M. A.; Forrest, S. R.; Kwong, R. U. S. Patent 20050214576, 2005.
(22) Chen, P.; Meyer, T. J. *Chem. Rev.* **1998**, *98*, 1439.
(23) Finkenzeller, W. J.; Hofbeck, T.; Thompson, M. E.; Yersin, H. *Inorg. Chem.* **2007**, *46*, 5076.
(24) Yersin, H.; Huber, P.; Wiedenhofer, H. *Coord. Chem. Rev.* **1994**, *132*, 35.
(25) Colombo, M. G.; Brunold, T. C.; Riedener, T.; Güdel, H. U.; Förtsch, M.; Bürgi, H.-B. *Inorg. Chem.* **1994**, *33*, 545.
(26) Endo, A.; Suzuki, K.; Yoshihara, T.; Tobita, S.; Yahiro, M.; Adachi, C. *Chem. Phys. Lett.* **2008**, *460*, 155.
(27) Gu, X.; Fei, T.; Zhang, H.; Xu, H.; Yang, B.; Ma, Y.; Liu, X. *J. Chem. Phys. A* **2008**, *112*, 8387.
(28) Finkenzeller, W. J.; Yersin, H. *Chem. Phys. Lett.* **2003**, *377*, 299.
(29) Harrigan, R. W.; Crosby, G. A. *J. Chem. Phys.* **1973**, *59*, 3468.
(30) Pentlehner, D.; Grau, I.; Yersin, H. *Chem. Phys. Lett.* **2008**, *455*, 72.
(31) Yersin, H.; Donges, D. *Top. Curr. Chem.* **2001**, *214*, 81.
(32) Yersin, H.; Finkenzeller, W. J. In *Highly Efficient OLEDs with Phosphorescent Materials*; Yersin, H., Ed.; Wiley-VCH: Weinheim, Germany, 2008, p 1.
(33) Yersin, H.; Strasser, J. *Coord. Chem. Rev.* **2000**, *208*, 331.
(34) Schäfer, H. L.; Gliemann, G. *Einführung in die Ligandenfeldtheorie; Akad. Verlagsgesellschaft: Wiesbaden* **1967**, p. 84.
(35) Orselli, E.; Kottas, G. S.; Konradsson, A. E.; Coppo, P.; Fröhlich, R.; De Cola, L.; van Dijken, A.; Büchel, M.; Börner, H. *Inorg. Chem.* **2007**, *46*, 11082.
(36) Djurovich, P. I., private communication.
(37) Ceulemans, A.; Vanquickenborne, L. G. *J. Am. Chem. Soc.* **1981**, *103*, 2238.
(38) Kober, E. M.; Meyer, T. J. *Inorg. Chem.* **1982**, *21*, 3967.
(39) Yersin, H.; Humbs, W.; Strasser, J. *Top. Curr. Chem.* **1997**, *191*, 153.
(40) Nozaki, K. *J. Chin. Chem. Soc.* **2006**, *53*, 101.
(41) Ikeda, S.; Yamamoto, S.; Nozaki, K.; Ikeyama, T.; Azumi, T.; Burt, J. A.; Crosby, G. A. *J. Phys. Chem.* **1991**, *95*, 8538.
(42) Abedin-Siddique, Z.; Ohno, T.; Nozaki, K.; Tsubomura, T. *Inorg. Chem.* **2004**, *43*, 663.
(43) Rausch, A. F.; Homeier, H. H. H.; Yersin, H. In *Topics in Organometallic Chemistry - Photophysics of Organometallics*; Lees A. J., Ed.; Springer: Berlin/Heidelberg, 2009.
(44) Daul, C.; Baerends, E. J.; Vernooijs, P. *Inorg. Chem.* **1994**, *33*, 3538.
(45) Kober, E. M.; Caspar, J. V.; Lumpkin, R. S.; Meyer, T. J. *J. Phys. Chem.* **1986**, *90*, 3722.
(46) Finkenzeller, W. J.; Thompson, M. E.; Yersin, H. *Chem. Phys. Lett.* **2007**, *444*, 273.
(47) Bauer, R.; Finkenzeller, W. J.; Bogner, U.; Thompson, M. E.; Yersin, H. *Org. Electron.* **2008**, *9*, 641.

JP902261C